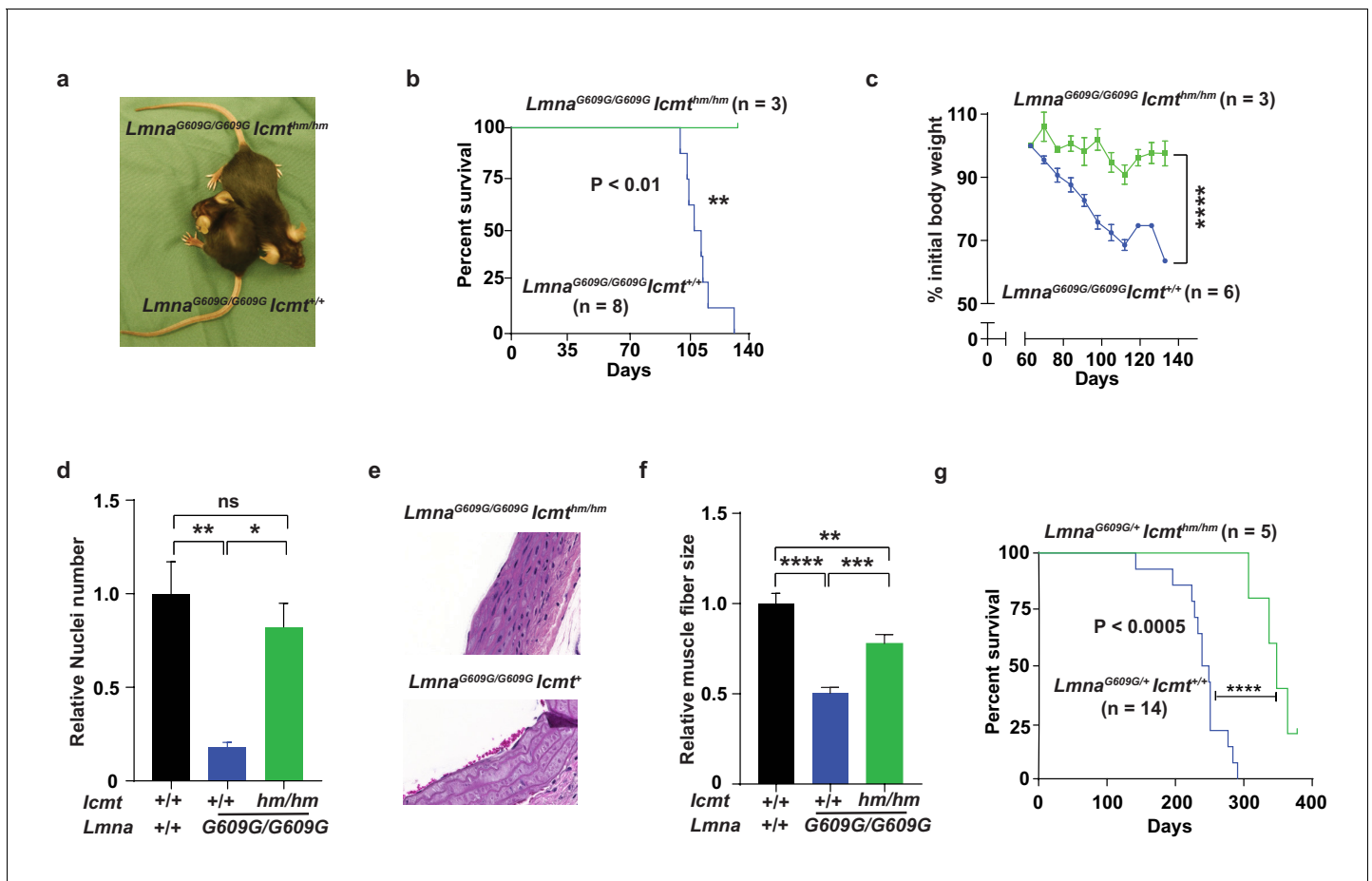


---

## Figures and figure supplements

A small-molecule ICMT inhibitor delays senescence of Hutchinson-Gilford progeria syndrome cells

**Xue Chen *et al***



**Figure 1.** Targeting *Icmf* improves survival and aorta and muscle phenotypes of progerin-knock-in mice. (a) Photograph of 15-week-old littermate female mice. (b) Kaplan-Meier plot showing survival of *Lmna*<sup>G609G/G609G</sup> *Icmf*<sup>hm/hm</sup> (n = 3) and *Lmna*<sup>G609G/G609G</sup> *Icmf*<sup>+/+</sup> (n = 8) mice; the three double-homozygotes were killed for analyses when all the control mice had died of progeria. (c) Body weight curves of mice in panel B. (d) Number of vascular smooth muscle cell nuclei in medial layer of aortic arch sections. Data are mean of three mice/genotype. (e) Representative photographs of aortic arch sections from panel d. (f) Skeletal muscle fiber cross-sectional diameter. Data are mean of 50 independent muscle cells diameters in *M. quadriceps extensor* from three mice/genotype. (g) Kaplan-Meier plot showing survival of *Lmna*<sup>G609G/+</sup> *Icmf*<sup>hm/hm</sup> (n = 5) and *Lmna*<sup>G609G/+</sup> *Icmf*<sup>+/+</sup> (n = 14) mice. \*p < 0.05; \*\*p < 0.01; \*\*\*p < 0.005; \*\*\*\*p < 0.001; n.s., not significant.

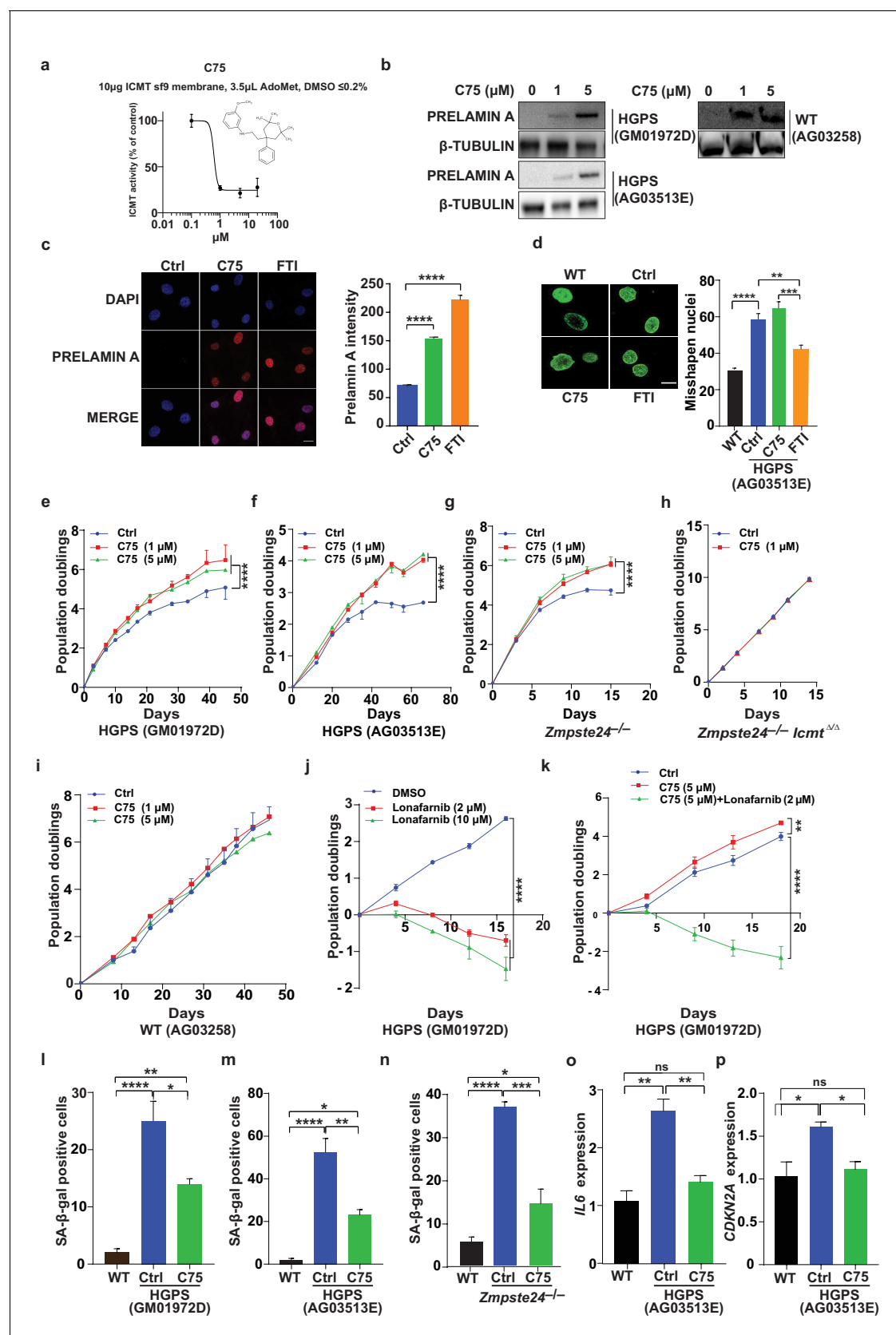


**Figure 2.** C75 inhibits isoprenylcysteine carboxylmethyltransferase (ICMT) activity and increases proliferation and reduces senescence of HGPS cells without affecting nuclear shape. (a) Chemical structure of compound 75 (C75) and percent ICMT activity remaining after incubation with C75. (b) Figure 2 continued on next page

## Figure 2 continued

Western blot showing increased amounts of prelamin A in Hutchinson-Gilford progeria syndrome (HGPS) and wild-type (WT) cells incubated with C75 for 20 days;  $\beta$  tubulin was the loading control. (c) Left, immunofluorescence images showing prelamin A expression in HGPS cells incubated with 5  $\mu$ M C75 for 20 days and 10  $\mu$ M farnesyltransferase inhibitor (FTI) for 3 days; the cells were counterstained with 4',6-diamidino-2-phenylindole (DAPI). Right, quantification of prelamin A staining intensity ( $n = 2$  cell lines and six individual images/cell line). (d) Left, representative nuclei of LAP2 $\beta$ -stained WT cells and HGPS cells incubated with vehicle (Ctrl), 5  $\mu$ M C75 for 20 days, and 10  $\mu$ M FTI for 3 days. Right, quantification of misshapen nuclei. Data are mean of  $\sim 1000$  nuclei and two independent experiments per cell line and condition. (e–h) Population doubling assays of late-passage HGPS cell lines (e, f), primary *Zmpste24* $^{-/-}$  mouse fibroblasts (g), and *Zmpste24* $^{-/-}$ *Lcmt* $^{-/-}$  fibroblasts (h) incubated with vehicle (Ctrl) and C75. (i) Population doubling of WT cells incubated with C75. (j, k) Population doubling assays of a late-passage HGPS cell line incubated with vehicle (Ctrl), lonafarnib, C75, and both drugs. (l–n) Senescence-associated beta-galactosidase ( $\beta$ -gal) staining of WT, HGPS, and *Zmpste24* $^{-/-}$  fibroblasts incubated with vehicle (Ctrl) and C75 for 20 days. (o, p) Interleukin 6 (*IL-6*) (o) and *CDKN2A* (p) expression in cells from experiment in panel m. \*\* $p < 0.01$ ; \*\*\* $p < 0.001$ ; \*\*\*\* $p < 0.0001$ ; n.s., not significant.

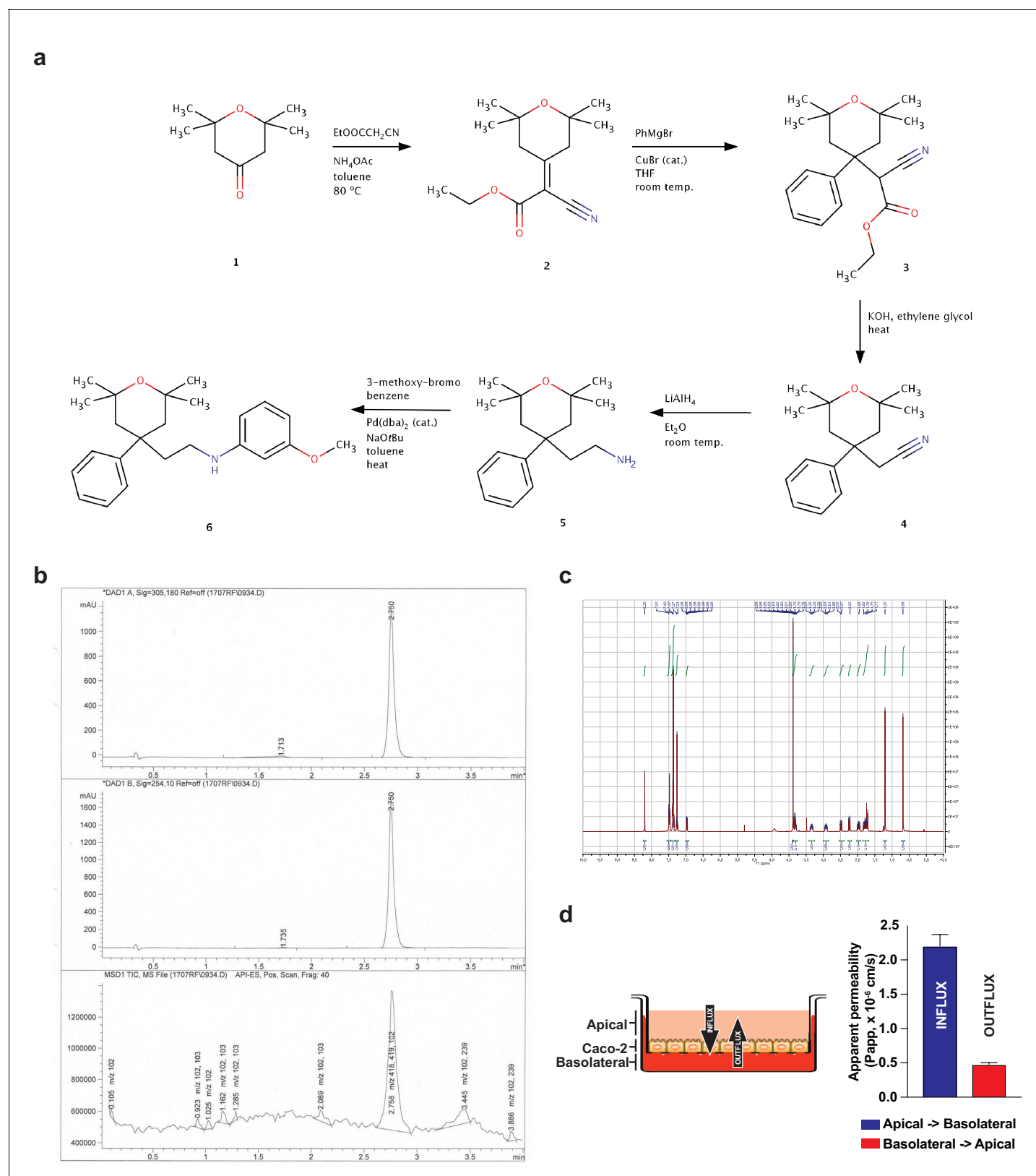


**Figure 2—figure supplement 1.** C75 synthesis and absorption, distribution, metabolism, and excretion (ADME) test. (a) Schematic of the C75 synthesis reactions. (b) Mass spectra of the final product. (c) Nuclear magnetic resonance spectra of C75. (d) Left, schematic of the apparent permeability assay through a layer of Caco-2 cells. Right, quantification of apical-to-basolateral (blue) and basolateral-to-apical (red) absorption rates across a Caco-2 cell layer.

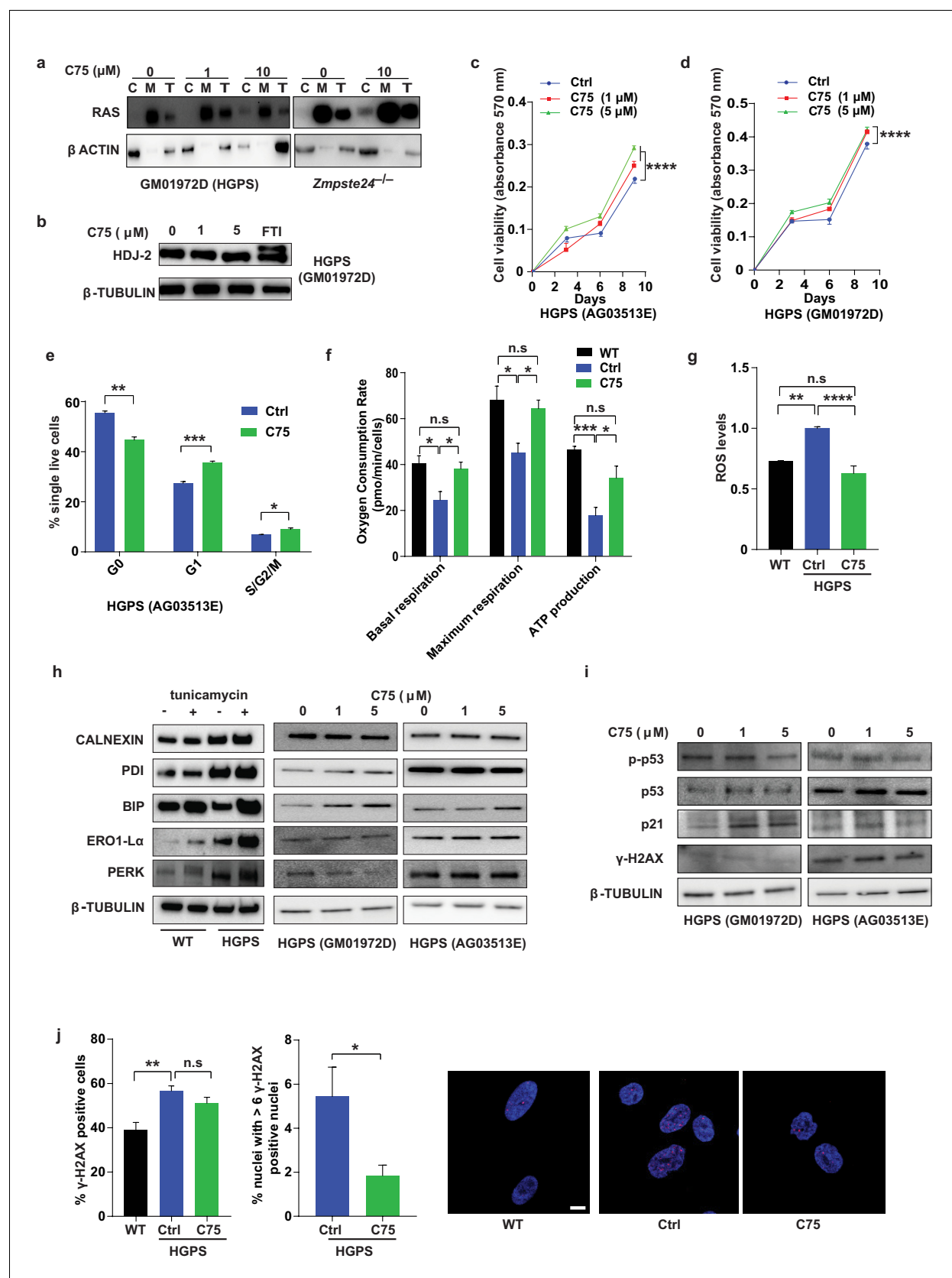


**Figure 2—figure supplement 2.** C75 increases viability, proliferation, and metabolic rates of Hutchinson-Gilford progeria syndrome (HGPS) cells and reduces reactive oxygen species (ROS) levels and nuclei with high levels of DNA damage. (a) Western blots showing levels of the RAS oncogene in total RAS and  $\beta$  ACTIN in GM01972D (HGPS) and *Zmpste24*<sup>-/-</sup> cells treated with C75 (0, 1, 10  $\mu$ M). **Figure 2—figure supplement 2 continued on next page**

*Figure 2—figure supplement 2 continued*

lysates (T) and in cytosolic (C) and membrane (M) fractions of late-passage HGPS cells and primary *Zmpste24*<sup>-/-</sup> mouse fibroblasts;  $\beta$ -actin was the loading control for cytosolic and total fractions. (b) Western blots showing electrophoretic mobility of the CAAX-protein HDJ2; a farnesyltransferase inhibitor (3-day incubation), but not C75 (20-day incubation), could partially reduce HDJ2 mobility. (c and d) Growth curves from presto blue-based cell viability assays of two HGPS cell lines. (e) Cell cycle analysis of HGPS cells. Data are mean of six technical replicates. (f) Seahorse analyses of basal and maximal respiration, and ATP production. Data are mean of two HGPS cell lines assayed in triplicate. (g) ROS levels in two HGPS cell lines incubated with C75 for 20 days. (h) Western blots showing levels of endoplasmic reticulum stress markers in lysates of two HGPS cell lines incubated with C75 for 20 days; tunicamycin was used as positive control. (i) Western blots showing levels of DNA damage markers in lysates of two HGPS cell lines incubated with C75 for 20 days. (j) Left, quantification of the frequency of  $\gamma$ -H<sub>2</sub>AX-positive nuclei in wild-type cells and in HGPS cells lines incubated with 5  $\mu$ M C75 for 20 days. Middle, quantification of nuclei with more than six  $\gamma$ -H<sub>2</sub>AX-foci HGPS cells incubated with 5  $\mu$ M C75 for 20 days. Data are mean of two cell lines and triplicate analyses. Right, immunofluorescence images showing  $\gamma$ -H<sub>2</sub>AX-positive nuclei (red); the nuclei were counterstained with DAPI (blue). \* $p < 0.05$ ; \*\* $p < 0.01$ ; \*\*\* $p < 0.001$ ; n.s., not significant.

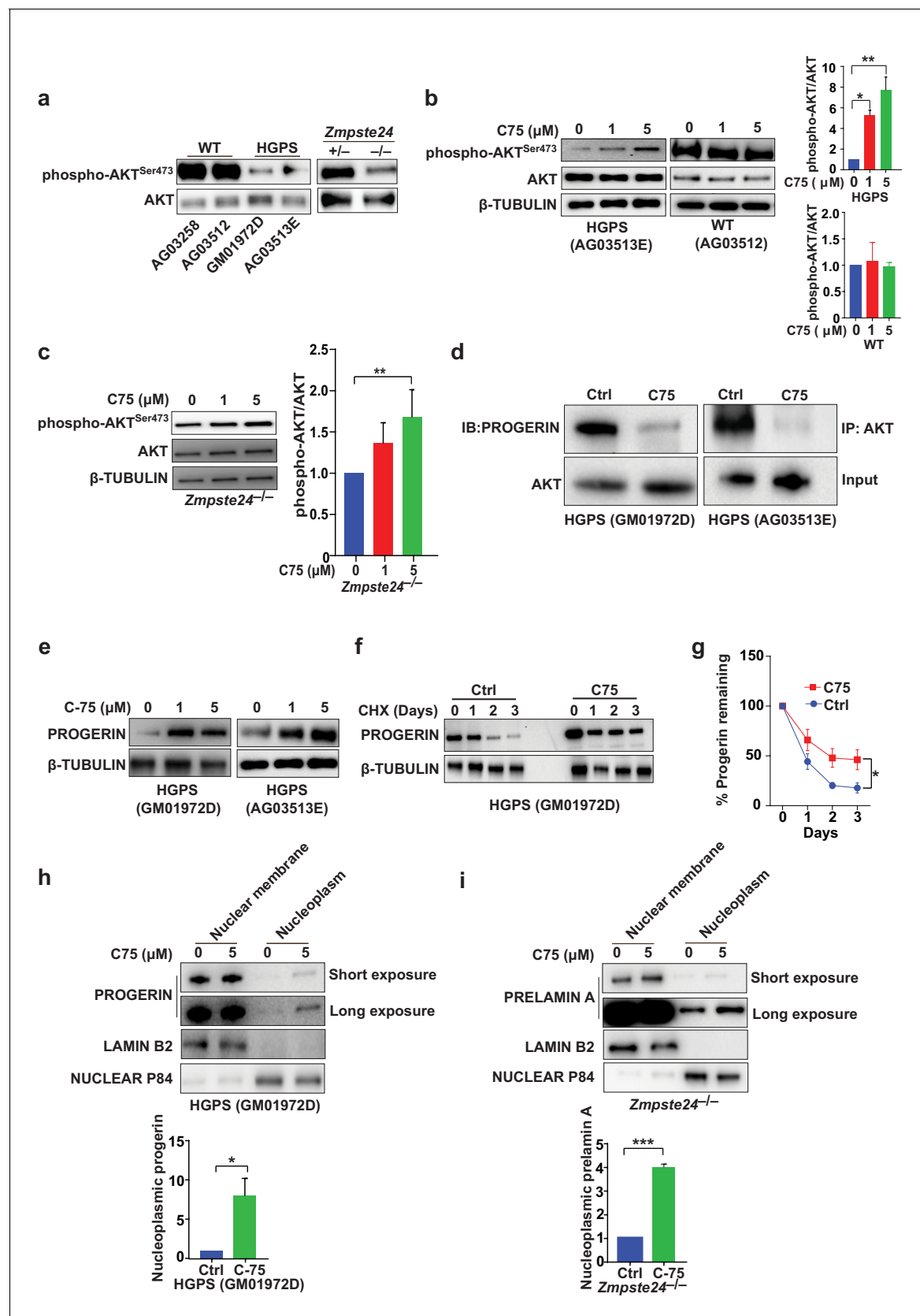


**Figure 3.** The isoprenylcysteine carboxylmethyltransferase inhibitor C75 disrupts progerin-AKT interactions, increases AKT activation, and mislocalizes progerin from the nuclear membrane to the nucleoplasm. (a) Western blot showing amounts of phosphorylated and total AKT (a.k.a protein kinase B) in

Figure 3 continued on next page



## Figure 3 continued

whole-cell lysates of human wild-type (WT) and Hutchinson-Gilford progeria syndrome (HGPS) cells and mouse *Zmpste24*-deficient fibroblasts. (b, c) Left panels, western blots (WB) showing amounts of phosphorylated and total AKT in WT and HGPS cells (b) and *Zmpste24*-deficient (c) fibroblasts incubated with C75 for 20–30 days;  $\beta$  tubulin was the loading control. Right panels, quantification of the ratio of phosphorylated and total AKT from densitometry analyses of protein bands. Data are mean of two independent cell lines, each analyzed in duplicate. (d) Immunoprecipitation (IP) and WB analyses showing that C75 disrupts the association between AKT and progerin. The lysates were also used directly for WB with total AKT antibodies (input). (e) WB showing amounts of progerin in HGPS cells incubated with C75 for 20 days. (f) WB showing amounts of progerin remaining in HGPS cells incubated with vehicle and 5  $\mu$ M C75 for 20 days and then with cycloheximide to stop protein synthesis. (g) Quantification of progerin amounts from the experiment in panel f and two others like it. (h, i) Left panels, WB showing amounts of progerin and prelamin A in nuclear membrane and nucleoplasm fractions of HGPS (h) and *Zmpste24*-deficient (i) fibroblasts, respectively, incubated with vehicle and 5  $\mu$ M C75 for 20 days. Lamin B2 and nuclear P84 were loading controls for nuclear membrane and nucleoplasm fractions, respectively. Right panels, quantification of nucleoplasmic progerin/prelamin A from densitometry analyses. \* $p < 0.05$ ; \*\* $p < 0.01$ ; \*\*\* $p < 0.001$ .